

Influence of Reaction Pressure on Semibatch Esterification Process of Poly(ethylene terephthalate) Synthesis

Himanshu Patel,^{1*} Gunter Feix,² Reinhard Schomäcker¹

Summary: Influence of esterification pressure on oligomeric properties was studied by using a semibatch reactor. Esterification model for semibatch process was further improved by considering EG reflux in the column. It was observed that increasing the reaction pressure decreases EG/water ratio in the column while increasing the EG/TPA feed ratio increases EG/water ratio in the column. By controlling the EG reflux in a semibatch reactor, it is possible to generate oligomers with similar oligomeric properties observed at different stages of continuous process.

Keywords: carboxyl groups; esterification; modeling; PET; pressure

Introduction

Poly(ethylene terephthalate) (PET) is considered as a very important polymer in commodity polymers after polyolefin. PET is mostly used for fibers, bottles, and films. PET is mainly synthesized from terephthalic acid (TPA) and ethylene glycol (EG) and the production of PET essentially involves three steps: direct esterification, prepolymerization, melt polycondensation. During the esterification process, water is continuously removed as a byproduct to form low molecular weight oligomers where the latter (chain length of 1–10) are conveyed to the prepolymerization step and subsequently to the final melt polymerization. In the semibatch esterification process, reaction temperature is increased gradually with the formation of oligomers and the vapors emerging from the reactor are passed through distillation column to separate water from EG and mainly EG is refluxed back to the reactor. In the

presented work, we have studied the influence of reaction pressure on EG reflux and subsequently its effect on oligomeric properties such as carboxyl group, EG consumption, chain length (n), esterification conversion (ϵ) and diethylene glycol (DEG) formation. Although, several mathematical models [1–3] for continuous esterification process have been published, in which influence of esterification pressure on oligomeric properties have been presented; however, a little has been reported for the influence of reaction pressure on a semibatch esterification process. Patel et al.^[4] have studied the influence of TPA particle size and EG/TPA feed ratio on the oligomeric properties by simulation for a semibatch reactor. In the current work, influence of pressure above atmosphere are estimated by simulation using the model^[4] whose validity was confirmed by several experiments in a semibatch reactor.

Mathematical Model

Reaction Scheme

Proton catalyzed esterification, polycondensation and etherification reactions are considered in this study. Functional group approach is considered for the simulation to

¹ Technical University of Berlin, Institute of Chemistry, Chemical Engineering Group, Sekr. TC 8, Strasse des 17. Juni 124–128, D-10623 Berlin, Germany

E-mail: himaqaoc@mailbox.tu-berlin.de

² Equipolymers GmbH, A Dow and PIC Joint Venture, Building F-17, D-06258 Schkopau, Germany

Table 1.
Molecular structures of components considered.

Symbol	Description	Molecular structure
a_F	Carboxyl group in terephthalic acid	
a_T	Carboxyl group attached to ester chain end	
b_F	Hydroxyl group in ethylene glycol	$\text{HOCH}_2\text{CH}_2\text{OH}$
b_T	Hydroxyl group attached to ester chain end	$\text{HOCH}_2\text{CH}_2\text{O}~$
w	Water	H_2O
d_T	Diethylene glycol bound at ester chain end	$\text{HOCH}_2\text{CH}_2\text{OCH}_2\text{CH}_2\text{O}~$
d_i	Internal ether link	$~\text{COOCH}_2\text{CH}_2\text{OCH}_2\text{CH}_2\text{OOC}~$
e_i	Internal ester group	
y	b_T or a_T	

Table 2.
Reaction scheme of the esterification process.

Reactions	Rate constants (forward, reverse)
$a_F - a_F + b_F - b_F \xrightleftharpoons[k_{E1}/K_1]{k_{E1}} a_T - b_T + w$	$k_{E1}, k_{E1}/K_1$
$a_F - a_F + b_T \text{~} y \xrightleftharpoons[k_{E2}/K_2]{k_{E2}} a_T \text{~} e_i \text{~} y + w$	$k_{E2}, k_{E2}/K_2$
$b_F - b_F + a_T \text{~} y \xrightleftharpoons[k_{E1}/K_1]{k_{E1}} b_T \text{~} y + w$	$k_{E1}, k_{E1}/K_1$
$y \text{~} a_T + b_T \text{~} y \xrightleftharpoons[k_{E2}/K_2]{k_{E2}} y \text{~} e_i \text{~} y + w$	$k_{E2}, k_{E2}/K_2$
$y \text{~} b_T + b_T \text{~} y \xrightleftharpoons[k_T/K_T]{k_T} y \text{~} e_i \text{~} y + b_F - b_F$	$k_T, k_T/K_T$
$y \text{~} b_T + b_T \text{~} y \xrightarrow{k_{ET}} y \text{~} d_i \text{~} y + w$	k_{ET}

Table 3.Reaction rate laws. (Reactions R_6 and R_7 produce DEG link).

Reaction rate laws
$R_1 = k_{E1} \cdot a_F \cdot b_F - (k_{E1}/K_1) \cdot b_T \cdot w$
$R_2 = k_{E2} \cdot a_F \cdot b_T - (k_{E2}/K_2) \cdot e_i \cdot w$
$R_3 = k_{E1} \cdot b_F \cdot a_T - (k_{E1}/K_1) \cdot b_T \cdot w$
$R_4 = k_{E2} \cdot a_T \cdot b_T - (k_{E2}/K_2) \cdot e_i \cdot w$
$R_5 = k_T \cdot b_T \cdot b_T - (k_T/K_T) \cdot e_i \cdot b_F$
$R_6 = k_{ET} \cdot b_T \cdot b_T$
$R_7 = k_{ET} \cdot b_F \cdot b_T$

determine end groups and byproducts effectively. Functional group description and reactions scheme are given in Table 1 and Table 2, respectively. In this study, the fourth order Runge-Kutta method was used to solve differential equations numerically applying Berkeley Madonna software package.

The assumptions for modeling were: (1) Reactions occur only in liquid phase. TPA is partially dissolved in the reaction mixture and only dissolved TPA takes part in the reaction. (2) TPA dissolution rate depends on TPA particle size (i.e. specific surface) and particles are assumed to be spherical for simplifications. (3) Solubility of TPA in water is negligible. (4) Only undissolved TPA forms solid phase of heterogeneous system. (5) Esterification reactions are catalyzed by protons which are generated by dissociation of terminal carboxyl groups of dissolved TPA ($a_{F,D}$) and carboxyl groups at ester ends (a_T). (6) Equal reactivity

is considered for carboxyl groups bound to TPA and to polymer chain while hydroxyl groups bound to EG and to terminal esters have different reactivity.^[5,6]

Reaction Rate

Reaction rate law for each component based on reaction scheme given in Table 2 is given in Table 3. Bimolecular reaction of TPA and EG converts one of the carboxyl groups (a_F) of TPA into the terminal ester group and the other in the terminal carboxyl group (a_T). The same is true for EG, where one of the hydroxyl groups (b_F) is converted into terminal ester group and the other in the terminal hydroxyl group (b_T). Consequently, factor of two is used for a_F and b_F in Table 4 to balance the reactions. Furthermore, esterification reactions between a_F and b_T , a_T and b_T and polycondensation reaction between b_T and b_T produce internal ester link (e_i). These properties are molality (mol/kg solvent) whereas the mass of total liquid phase can be represented as the solvent mass. Therefore, the use of the unit mol/kg means: moles of terminal or internal functional groups per mass of total liquid phase.

Phase Equilibrium

Due to the limited solubility of TPA in EG and the esterification is occurring in liquid phase only; the solid-liquid equilibrium is considered to calculate the functional groups concentration. In simulation, TPA

Table 4.

Mass balance equations.

Equations
$\frac{da_F}{dt} = -2 \cdot R_1 - 2 \cdot R_2$
$\frac{db_F}{dt} = -2 \cdot R_1 - 2 \cdot R_3 + 2 \cdot R_5 - 2 \cdot R_7 - k_{v,EG} \left(b_{F,L} - 2 \cdot \frac{\gamma_{EG(z)} N_L^s}{\left(\frac{p_{EG}}{p}\right)^{z+1} \gamma_{EG}^s \prod_{z=0}^z \gamma_{EG(z)}} \right)$
$\frac{da_T}{dt} = +R_1 + R_2 - R_3 - R_4$
$\frac{db_T}{dt} = +R_1 - R_2 + R_3 - R_4 - 2 \cdot R_5 - 2 \cdot R_6 - R_7$
$\frac{dw}{dt} = +R_1 + R_2 + R_3 + R_4 + R_6 + R_7 - k_{v,w} \left(w_L - \frac{\gamma_{W(z)} N_L^s}{\left(\frac{p_W}{p}\right)^{z+1} \gamma_W^s \prod_{z=0}^z \gamma_{W(z)}} \right)$
$\frac{d(e_i + d_i)}{dt} = +R_6 + R_7$

solubility in EG and oligomers is considered according to Yamada et al.^[2] TPA solubility in EG is given as:

$$\beta_{\text{TPA,EG}} = 9062 \exp[-4877/T] \text{mol} \cdot \text{kg}^{-1} \quad (1)$$

TPA solubility in oligomers is given as:

$$\beta_{\text{TPA,OLG}} = 374 \exp[-3831/T] \text{mol} \cdot \text{kg}^{-1} \quad (2)$$

where T is the temperature in K

Maximum TPA solubility in the EG and oligomers, a_F^* can be calculated by using Equation (1), (2), (4), (5) and the esterification conversion, ε (for definition see Equation (26)).

$$a_F^* = \beta_{\text{EG}} + \varepsilon \cdot (\beta_{\text{OLG}} - \beta_{\text{EG}}) \text{mol} \cdot \text{kg}^{-1} \quad (3)$$

The solubility of TPA in terms of carboxyl groups in EG,

$$\beta_{\text{EG}} \equiv 2 \cdot \beta_{\text{TPA,EG}} \text{mol} \cdot \text{kg}^{-1} \quad (4)$$

The solubility of TPA in terms of carboxyl groups in oligomers,

$$\beta_{\text{OLG}} \equiv 2 \cdot \beta_{\text{TPA,OLG}} \text{mol} \cdot \text{kg}^{-1} \quad (5)$$

Reaction rate for total carboxyl groups (a) can be given as,

$$\frac{da}{dt} = \frac{da_{F,S}}{dt} + \frac{da_{F,D}}{dt} + \frac{da_T}{dt} \quad (6)$$

Where, $a_{F,S}$ represents the carboxyl groups attached to undissolved TPA. Carboxyl groups become available by TPA dissolution in the liquid phase and consumed by esterification reaction. It is assumed that the change of $a_{F,D}$ in the presence of $a_{F,S}$ is close to zero.

$$\begin{aligned} \frac{da_{F,D}}{dt} &= \frac{da_{F,S}}{dt} - R_1 - R_2 \\ &= \underbrace{k_D \cdot (a_F^* - a_{F,D})}_{\text{dissolution}} - \underbrace{R_1 - R_2}_{\text{consumption}} \\ &\approx 0 \end{aligned} \quad (7)$$

The mass transfer coefficient k_D depends on the TPA particle specific surface. k_D is calculated based on TPA particle size

distribution and particle specific surface according to Patel et al.^[4]

Vapor-liquid phase equilibrium is considered based on polymer-NRTL parameters obtained from ASPEN databank.^[7] EG and water are considered only volatile components while oligomers and DEG are considered to be non volatile under used reaction conditions. The mole fractions and activity coefficient are calculated based on apparent amount of water, EG and oligomers in the liquid phase. The vapor phase mole fractions of EG and water are given by the following equations.

$$y_{\text{EG}} \cdot \gamma_{\text{EG}} \cdot P_{\text{EG}} = y_{\text{EG}} \cdot P \quad (8)$$

$$x_w \cdot \gamma_w \cdot P_w = y_w \cdot P \quad (9)$$

$$x_{\text{DEG}} + x_{\text{EG}} + x_w + x_{\text{OLG}} = 1 \quad (10)$$

$$y_{\text{EG}} + y_w = 1 \quad (11)$$

where, x_{DEG} , x_{EG} , x_w and x_{OLG} are the liquid phase apparent mole fraction of DEG, EG, water and oligomers, y_{EG} and y_w are the vapor phase mole fractions of EG and water, P_{EG} and P_w are the vapor pressure of pure EG and pure water in bar, P is the total pressure in bar, and γ_{EG} and γ_w are the activity coefficient of EG and water. Vapor pressures of pure components are calculated from Yamada et al.^[2]

$$\begin{aligned} \log P_{\text{EG}} &= 7.8808 + \log(1/750) \\ &\quad - 1957/(\vartheta + 193.8) \end{aligned} \quad (12)$$

$$\begin{aligned} \log P_w &= 7.9668 + \log(1/750) \\ &\quad - 1668.2/(\vartheta + 228) \end{aligned} \quad (13)$$

where, ϑ is the reaction temperature in °C

In Table 4, a simple approach has been considered for the mass balance equations for EG and water. The terms for water and EG removal as condensate were derived by considering the water and EG separation without column, within column and with column. The model equations for each situation are given as follow,

EG and Water Separation without Column

$$w_L^* = \frac{N_L^*}{m_L} x_w^* = \frac{N_L^*}{m_L} y_w \frac{P}{P_w \gamma_w^*} \quad (14)$$

w_L^* is a molality of water in the melt at boundary layer. N_L^* is the total moles of the reactive components in the melt at boundary layer. The total number of moles at this position should be comparable as the total number of moles in the bulk phase N_L .

$$N_L^* \approx N_L = m_L (w_L + (b_{F,L}/2) + (a^\circ/2n)) \quad (15)$$

where w_L and $b_{F,L}$ represents the moles of water and b_F in liquid phase. m_L is the mass of liquid phase which can be given as,

$$m_L = n_{a(0)}/a^\circ \quad (16)$$

where $n_{a(0)}$ are the initial moles of carboxylic acid groups and a° is the saponification number. x_w^* is the mol fraction of water in the melt at boundary layer and γ_w^* is the activity coefficient of water in the melt at boundary layer. (calculated as per ASPEN PNRTL model)

EG and Water Separation within Column

For the column having z stages, EG and water separation within column can be given as,

$$\left[\frac{y_{w(z)}}{x_{w(z=0)}} \right] = \left[\frac{1 - y_{EG(z)}}{1 - x_{EG(z=0)}} \right] = \left(\frac{P_w}{P} \right)^z \prod_{z=0}^z \gamma_{w(at z)} \quad (17)$$

where $y_{w(z)}$ is the mole fraction of water in vapor phase at stage z , $x_{EG(z=0)}$ is the mole fraction of EG in the liquid phase at bottom of the column, $y_{EG(z)}$ is the mole fraction of EG in vapor phase at stage z , $x_{w(z=0)}$ is the mole fraction of water in the liquid phase at bottom of the column.

EG and Water Separation with Column

By combining Equation (14) and (17) and considering theoretical number of column stage $z = 2.2$ (measured by EG-water VLE-data); EG and water separation with

column can be given as,

$$w_L^* = \frac{N_L^*}{m_L} \frac{y_{w(z)}}{\left(\frac{P_w}{P} \right)^z \gamma_w^* \prod_{z=0}^z \gamma_{w(at z)}} \quad (18)$$

By simplifying the Equation (18), the relationship of w_L^* and $y_{w(z)}$ can be obtained as follow.

$$w_L^* = \frac{N_L^*}{m_L} \frac{y_{w(z)}}{\left(\frac{P_w}{P} \right)^{z+1} \gamma_w^* \prod_{z=0}^z \gamma_{w(at z)}} \quad (19)$$

Mass transfer coefficient of water ($k_{v,w}$) and EG ($k_{v,EG}$) is taken from Rafler et al.^[8] By using the mass transfer coefficient in Equation (19), the total transfer of water and EG from the respective bulk phases w_L and $b_{F,L}$ into the condensate ($y_{w(z)}$, $y_{EG(z)}$) is given by,

$$k_{v,w}(w_L - w_L^*) = k_{v,w} \left(w_L - \frac{y_{w(z)} N_L^*}{\left(\frac{P_w}{P} \right)^{z+1} \gamma_w^* \prod_{z=0}^z \gamma_{w(at z)}} \right) \quad (20)$$

$$k_{v,EG}(b_{F,L} - b_{F,L}^*) = k_{v,EG} \left(b_{F,L} - 2 \frac{y_{EG(z)} N_L^*}{\left(\frac{P_{EG}}{P} \right)^{z+1} \gamma_{EG}^* \prod_{z=0}^z \gamma_{EG(z)}} \right) \quad (21)$$

Catalysis

In the present study, the esterification reactions were studied without any metal catalysts. Esterification reactions involve acid catalysis mechanism. The catalytic influence of an acid depends on the degree of dissociation of the acid. Acid strength (pK_a) of dissolved TPA carboxyl group and oligomeric terminal carboxyl group are considered to be the same.^[9,10] The pK_a value of carboxyl group of TPA and terminal carboxyl groups is given in mol/L. From our experience, the density of the melt

Table 5.

Kinetic parameters used for the simulation.

Kinetic constants $k_{\infty,i} = A_i \exp(-E_i/RT)$	Activation energy E_i [kcal mol ⁻¹]	Frequency factor A_i [kg ² mol ⁻² min ⁻¹]	Equilibrium constant
$k_{\infty,E1}$	18	4.60×10^8	K_1 : 2.50
$k_{\infty,E2}$	18	1.06×10^{10}	K_2 : 1.25
$k_{\infty,T} = k_{\infty,E1}/3$			K_T : 0.5
$k_{\infty,ET}$	29.8	4.59×10^{12}	–

Table 6.

Numerical values used for the simulation.

- 1) $k_{v,w} = 0.438 \text{ min}^{-1}$
- 2) $k_{v,EG} = 0.156 \text{ min}^{-1}$
- 3) Theoretical number of stages (z) in the column = 2.2
- 4) $pKa = 3.51$

esterification phase is close to 1 kg/L. Therefore given Equation (22) can be used for the calculations where the molality has been considered.

$$H^+ \approx (a_{F,D} + a_T) \cdot 10^{-pKa} \quad (22)$$

The effective rate constant for esterification, polycondensation and DEG formation reactions can be given by,

$$k_i = H^+ \cdot k_{\infty,i} \quad (23)$$

where, $k_{\infty,i}$ is a micro kinetic rate constant

Otton et al.^[10] observed that acid catalyzed esterification is about three times faster than acid catalyzed polycondensation. This relationship is used for the polycondensation rate constant, $k_T = k_{ET}/3$.

Experimental Part

The direct esterification was carried out in a “Parr” semibatch reactor of a 1 liter reaction volume and equipped with magnetic stirrer drive. EG (1.82 mol) and TPA (1.3 mol) were mixed thoroughly to make paste and charged to the reactor. Reactor and the slurry were made oxygen free by applying nitrogen flush and vacuum simultaneously. Reactor was pressurized with nitrogen up to 2.5 bar. Installed column was of a straight reflux type with helix inner packing. The column temperature was maintained at

150 °C throughout the reaction to separate water and EG and to prevent the temperature drop due to EG reflux. The condenser temperature and stirrer speed was set to –4 °C and 140 rpm respectively. Oil temperature was set to 290 °C. With the increase of the reaction temperature, the pressure was increased simultaneously and controlled with magnetic pressure valve. Pressure was maintained constant throughout the experiment at desired set value. At the early phase of esterification, the reaction temperature increased to the boiling point of EG at given pressure and as the reaction progressed, oligomers were being formed and reaction temperature also increased due to increase of the boiling point of reaction phase. Resulting reaction temperature increased from 230 to 260 °C. After 90 minutes, the pressure was gradually reduced to the atmospheric pressure in 5 minutes and the condensate mixture (water + EG) was collected and analyzed. At the same time, the esterified oligomers were removed from the reactor and quenched in dry ice. Oligomers were analyzed for their molecular weight and carboxyl groups’ concentration. Several experiments were carried out with different set pressure in the range between 3 to 3.75 bar to study its influence on oligomeric properties.

Intrinsic viscosity of oligomers, carboxyl groups and water in reaction byproduct mixture were determined by the methods given in Patel et al.^[4]

DEG Determination

About 1g of the oligomeric sample was added together with 30 ml methanol and

zinc acetate as catalyst and tetra ethylene glycol dimethyl ether as internal standard into a pressure container. The container was heated for two hours at 220 °C in an oven to decompose the oligomers to the DEG and methyl isophthalate. The sample mixture was cooled to the room temperature and analyzed by gas chromatography (PERKIN ELMER GC – Autosystem XL). The DEG contents were calculated from the areas of the DEG peak in relation to the internal standard peak.

Results and Discussion

In semibatch or continuous PET process, the degree of polymerization advances by esterification and polycondensation reactions simultaneously. Therefore, it is important to have the optimum balance of carboxyl and hydroxyl group to attain optimum conversion. An excess or deficiency of one or the other reactant will cause quality deviations and the changes in the reaction rate.^[11]

In semibatch process, esterification phase is nearly completed before applying full vacuum to initiate polycondensation phase. Therefore, at the beginning of batch polycondensation, oligomeric fraction of carboxyl groups in total terminal groups (α) remains significantly lower than in continuous process. While, in continuous process, the carboxyl group concentration changes at different stages due to their consumption via esterification and formation via ester link degradation reactions. In most indus-

trial continuous processes, the melt-phase reaction is performed in three to five continuous reactors in series.^[12] Therefore, it is desirable to have specific oligomeric α at every stage to fulfill the requirement of next stage in continuous process.

Yokoyama^[13] and Duh et al.^[14] studied the effect of carboxyl group concentration on polycondensation rate in melt and solid phase respectively. However, the formation of oligomers with α having broad values and its effect on esterification and polycondensation rate has not been studied extensively. As far as we know, there has not been a paper narrating the generation of oligomers of different α by a semibatch process that resembles the oligomers observed at the different stages of a continuous process. In this paper, we have made an attempt to simulate continuous process functional group profile by using semi batch process. In our previous studies^[4], we generated the oligomers of different α values by varying the EG/TPA feed ratio. However, the obtained α value was observed to be lower than in continuous process. The feed ratio could not be lowered further due to extremely low solubility of TPA in EG. In presented work, we have generated oligomers of different α by varying the esterification pressure at constant EG/TPA feed ratio.

Influence of Esterification Pressure on EG Reflux

Figure 1 shows the influence of esterification pressure on fraction of unreacted EG

Table 7.

Experimental results of esterified oligomers under varied pressure.

P	t	EG/TPA	(EG _o -EG _R)/EG _o	a _T	b _T	Mn	n	α	ε	p	DEG
bar	min	mol/mol		mol kg ⁻¹	mol kg ⁻¹	g mol ⁻¹					wt. %
3.13	95	1.4	0.28	0.70	0.77	1355	6.95	0.48	0.962	0.790	3.1
3.13	95	1.4	0.29	0.75	0.68	1401	7.21	0.52	0.897	0.840	
3.22	95	1.4	0.28	0.68	0.80	1346	6.90	0.46	0.932	0.856	
3.22	95	1.4	0.27	0.64	0.86	1335	6.82	0.43	0.954	0.842	3.4
3.34	95	1.4	0.24	0.47	1.13	1250	6.32	0.29	0.961	0.821	3.7
3.50	95	1.4	0.20	0.43	1.68	948	4.71	0.20	0.933	0.855	
3.55	95	1.4	0.21	0.39	1.40	1116	5.59	0.22	0.938	0.853	4.5
3.55	95	1.4	0.19	0.31	1.58	1060	5.27	0.16	0.927	0.861	
3.75	95	1.4	0.19	0.37	1.71	959	4.76	0.18	0.969	0.810	4.9

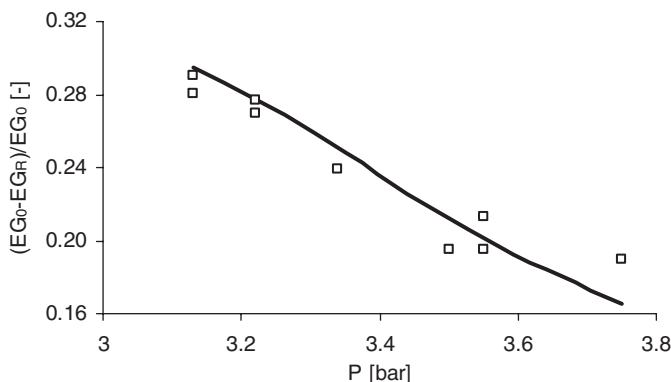


Figure 1.

Effect of esterification pressure on unreacted EG in vapour and liquid phase. Symbols: experimental values; Line: calculated.

to initial EG feed. This fraction can be calculated as,

$$EG^L + EG^V = EG_0 - EG_R$$

$$= EG_0 - \frac{a^0 \cdot (2 \cdot \varepsilon - p) \cdot m_L}{2} \quad (24)$$

where, EG^L and EG^V are the moles of unreacted EG in liquid and vapor phase respectively. EG_0 and EG_R are the moles of initial and reacted EG respectively. ε and p are the esterification conversion and conversion by chain propagation respectively.

Unreacted EG at the end of esterification phase can be calculated by using

Equation (24) which simplifies the influence of pressure on EG reflux. As can be seen in Figure 1, an increase in esterification pressure boosts EG consumption and thus lowers unreacted EG. Furthermore, to investigate the influence of pressure and EG/TPA feed ratio on vapor phase composition, condensate was collected at the end of esterification and analysed for EG and w content. From Figure 2, it can be seen that increasing pressure reduces EG/w ratio in the vapor phase by increasing the EG reflux. From Figure 3, it is seen that EG/w ratio in the vapor phase exhibits some opposite behaviour with increasing EG/TPA feed ratio. This is due to the increasing

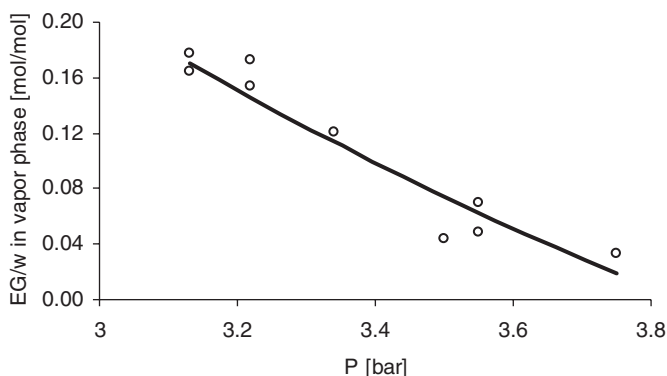
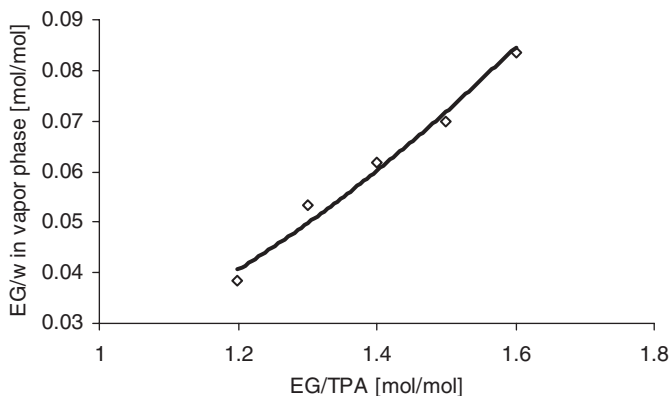


Figure 2.

Effect of esterification pressure on EG/W in vapor phase. Symbols: experimental values; Line: calculated.

**Figure 3.**

Effect of EG/TPA feed ratio on EG/W in vapor phase. Pressure: 4 bar.

EG mol fraction in liquid phase enhances EG mol fraction in vapor phase.

From Figure 4 it can be seen that lowering the pressure in esterification phase decreases the EG reflux and reduces the EG concentration in liquid phase. Reduction of excess EG in liquid phase promotes further esterification of a_T with b_T and also lowers reverse polycondensation reaction which is responsible to increase n and α . Figure 4 suggests that it is possible to prepare oligomers having α value of a broad range by varying the EG reflux or the reaction pressure instead of varying the EG/TPA feed ratio. n was calculated from the measured intrinsic viscosity using Equation (25).^[4]

$$n = (\overline{M}_n - 62 + 88 \cdot \alpha) / 192 \quad (25)$$

where $\overline{M}_n = 3.27 \times 10^4 \cdot IV^{1.4706}$.

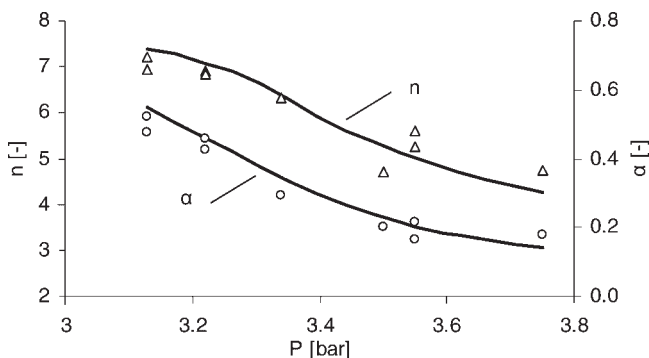
Figure 5 supports that higher reaction pressure increases the EG concentration in liquid phase which promotes both esterification and etherification and thus overall EG consumption was observed to be enhanced. DEG formation was observed much higher than commercial continuous process. This was expected due to higher reaction pressure and reactions carried without any DEG suppressant.

Esterification conversion ε , which represents conversion of TPA into esters, can be expressed as,

$$\varepsilon = 1 - \frac{a}{a^\circ} \quad (26)$$

While conversion by chain propagation (p) can be given as,

$$p = 1 - \frac{E}{a^\circ} = 1 - \frac{a + b_T}{a^\circ} \quad (27)$$

**Figure 4.**

Effect of esterification pressure on n and α . Symbols: experimental values; Line: calculated.

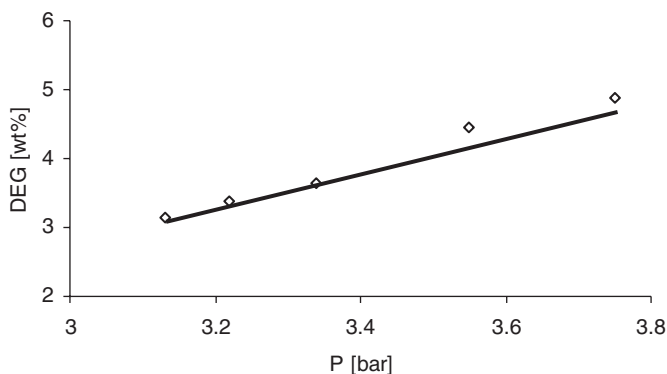


Figure 5.

Influence of reaction pressure on DEG formation. Symbols: experimental values; Line: calculated.

where, E is total terminal groups.

From Figure 6 it is seen that higher reaction pressure increases the esterification conversion due to higher concentration of EG in liquid phase which enhances the TPA dissolution and consequently its conversion through esterification reaction. While, pressure has significant effect on EG reflux which influence the carboxyl to hydroxyl ratio in the reaction liquid phase. Thus, deviation from optimum functional group balance reduces p .

Conclusion

Esterification pressure has similar influence as the EG/TPA feed ratio on certain

oligomeric properties. An increase in both variables enhances esterification conversion (ϵ) and decreases the chain propagation conversion (p). However, it was observed that by increasing the reaction pressure, EG/w ratio in the vapor phase was observed to be decreased while by increasing the EG/TPA feed ratio, EG/w ratio in the vapor phase was observed to be increased. It has been shown that by varying the reaction pressure in a semibatch esterification process, it is possible to produce oligomers of α having a broad range that observed in continuous process. Semibatch process can be utilized to study different additives and catalysts in the presence of functional groups profile observed in continuous process.

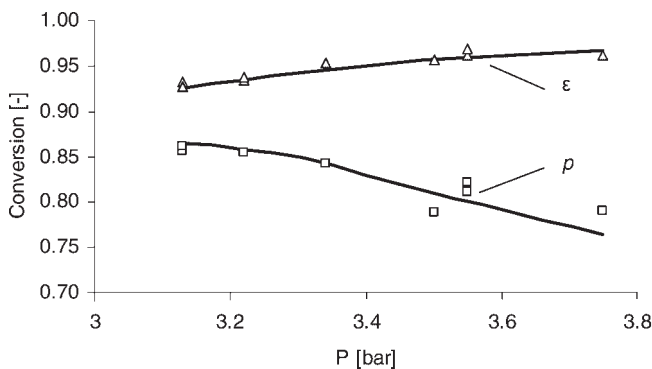


Figure 6.

Influence of reaction pressure on conversion. Symbols: experimental values; Line: calculated.

- [1] K. Ravindranath, R. Mashelkar, *Polym. Eng. Sci.* **1982**, 22, 10.
- [2] T. Yamada, *Polym. J.* **1992**, 24(1), 43.
- [3] C. K. Kang, B. C. Lee, D. W. Ihm, D. A. Tremblay, *J. App. Polym. Sci.* **1997**, 63, 163.
- [4] H. Patel, G. Feix, R. Schomaecker, *Macromol. React. Eng.* **2007**, 1, 502.
- [5] G. Challa, *J. Polym. Sci., Makromol. Chem.* **1959**, 38, 105.
- [6] J. Otton, S. Ratton, *J. Polym. Sci., Part A: Polym. Chem.* **1991**, 29, 377.
- [7] ASPEN databank, Aspen Technology, Inc.
- [8] G. Rafler, F. Herfurth, B. Otto, J. Marth, H. Gajewski, K. Zacharias, *Acta Polymerica*, **1989**, 40(1), 44.
- [9] H. C. Brown, “*Determination of Organic Structures by Physical Methods*”, E. A., Braude, F. C. Nachod, Eds., Academic Press, New York **1955**.
- [10] J. Otton, S. Ratton, *J. Polym. Sci. Part A: Polym. Chem.* **1988**, 26, 2183.
- [11] E. van Endert, R. Hagen, *Chemiefasern/Textilindustrie (CTI)*, **1993**, 42/95, 480.
- [12] Th. Rieckmann, S. Voelker, *Modern Polyesters*, J. Wiley & Sons, Ltd., 93, **2003**.
- [13] H. Yokoyama, T. Sano, T. Chijiwa, R. Kajiya, *Kobunshi Ronbunshu*, **1979**, 36(8), 557.
- [14] B. Duh, *J. App. Polym. Sci.* **2002**, 83, 1288.